

Discovery of novel inhibitors of the ZipA/FtsZ complex by NMR fragment screening coupled with structure-based design

Désirée H. H. Tsao,^{a,*} Alan G. Sutherland,^c Lee. D. Jennings,^c Yuanhong Li,^a Thomas S. Rush, III,^{a,†} Juan C. Alvarez,^{d,‡} Weidong Ding,^b Elizabeth G. Dushin,^c Russell G. Dushin,^c Steve A. Haney,^d Cynthia H. Kenny,^b A. Karl Malakian,^a Ramaswamy Nilakantan^a and Lidia Mosyak^a

^aStructural Biology and Computational Chemistry, Wyeth Research, Cambridge, MA 02140, USA

^bBiophysical Enzymology, Wyeth Research, Pearl River, NY 10965, USA

^cMedicinal Chemistry, Wyeth Research, Pearl River, NY 10965, USA

^dBiological Technologies, Wyeth Research, Cambridge, MA 02140, USA

Received 11 May 2006; revised 19 July 2006; accepted 26 July 2006

Available online 17 August 2006

Abstract—ZipA is a membrane anchored protein in *Escherichia coli* that interacts with FtsZ, a homolog of eukaryotic tubulins, forming a septal ring structure that mediates bacterial cell division. Thus, the ZipA/FtsZ protein–protein interaction is a potential target for an antibacterial agent. We report here an NMR-based fragment screening approach which identified several hits that bind to the C-terminal region of ZipA. The screen was performed by ¹H–¹⁵N HSQC experiments on a library of 825 fragments that are small, lead-like, and highly soluble. Seven hits were identified, and the binding mode of the best one was revealed in the X-ray crystal structure. Similar to the ZipA/FtsZ contacts, the driving force in the binding of the small molecule ligands to ZipA is achieved through hydrophobic interactions. Analogs of this hit were also evaluated by NMR and X-ray crystal structures of these analogs with ZipA were obtained, providing structural information to help guide the medicinal chemistry efforts.

© 2006 Elsevier Ltd. All rights reserved.

1. Introduction

Bacterial drug resistance is rapidly becoming a serious threat to global health, where many disease-causing microbes become resistant to drug therapy.¹ Part of this problem is the bacteria and other microorganisms that cause infections become remarkably resilient through mutations, and can develop ways to circumvent the action of drugs meant to kill or weaken them. In an effort to find new classes of antibiotics that will affect the bacterial cell cycle, we undertook the challenge to identify small molecule drug leads that would prevent *Escherichia coli* cell division by interfering with the protein/protein interaction ZipA/FtsZ.

Cell wall division in *E. coli* involves a complex series of events with the involvement of at least eight different proteins.^{2,3} One of the first steps in bacterial cell wall division involves the formation of the Z-ring, a circular polymeric structure formed by the cytosolic protein FtsZ.⁴ FtsZ is required for cell division in both Gram– and Gram+ bacteria, and is highly conserved among different species.⁵ It is one of the best conserved division proteins in its family and its role in cell division traces back very early in evolution.⁶ FtsZ is an α - and β -tubulin homolog as revealed by its crystal structure⁷ and upon binding to GTP polymerizes to form a ring-like structure at the division site.⁷ Sedimentation assays and yeast two hybrid experiments⁸ have shown that the C-terminus of FtsZ is responsible for binding to ZipA. In Gram-negative bacteria, ZipA is one of the first proteins recruited to the division site and binds to FtsZ,^{9,10} providing stability to the FtsZ ring from its involvement in both assembly and function of the septal ring structure. ZipA is a 328 aa protein which is comprised of several domains: the hydrophobic membrane-anchor N-terminus domain (aa 1–24), a highly charged

Keywords: NMR screening; ZipA/FtsZ inhibitor; Fragment-based drug discovery; X-ray structures.

* Corresponding author. Tel.: +1 617 665 5667; fax: +1 617 665 5682; e-mail: dsao@wyeth.com

† Present address: Merck Research Laboratories, Boston, MA, USA.

‡ Present address: J&J TransForm Pharmaceuticals, Lexington, MA 02421, USA.

domain (aa 25–84), a P/Q proline/glutamine-rich domain (aa 85–187), and the C-terminal domain (aa 188–328). The N- and C-terminal domains are highly conserved among different organisms,⁹ thus suggesting their importance in bacterial cell wall division. Binding studies performed by Hale et al.¹⁰ have shown that the last 143 residues (aa 186–328) are sufficient to interact with FtsZ, but not sufficient to support cell division.

The three-dimensional structure of the C-terminal of ZipA has been solved by X-ray crystallography and by NMR methods.^{11,12} ZipA is composed of a β -sheet packed against three α -helices, where the exposed site of the beta sheet forms a shallow cavity, formed mostly by hydrophobic residues.^{11,12} A 17-residue peptide from the C-terminus of FtsZ with sequence KEPDYLDIPAFLRKQAD was identified to bind to ZipA with an affinity of 7 μ M, and shown to compete with the full length FtsZ for binding to ZipA.¹² The details of the interaction between ZipA and the peptide have been revealed,¹² where two hydrophobic faces are buried together. The peptide binds to the exposed side of the β -sheet in ZipA, making mostly hydrophobic contacts in the cavity. Furthermore, mutational analysis on the peptide demonstrated that most of the binding interaction comes from three hydrophobic residues Ile, Phe, and Leu.¹² Indeed, the most extensively buried side chains are the hydrophobic residues Leu372, Ile374, Phe377, and Leu378 that fit tightly into the ZipA pocket.¹² Likewise in ZipA, eleven residues, most of which are hydrophobic and span all six β -strands in the protein, make contact with the peptide. The solvent accessible area buried upon binding is $\sim 1350 \text{ \AA}^2$. Polar interactions made adjacent to the tight hydrophobic binding pocket include a Phe-Arg π -type interaction, and two hydrogen bonds between main chain atoms of ZipA and FtsZ (FtsZ₃₇₀/ZipA₆₆ & FtsZ₃₇₂/ZipA₆₄).

In an effort to find a small molecule that would inhibit the ZipA/FtsZ interaction and thus interfere with bacterial cell division, a high throughput (HTS) screen and an NMR screen were performed. NMR-based screening is becoming a valuable complement to HTS screening.^{13,14} NMR libraries are generally comprised of a set of low molecular weight compounds. Through NMR screening, fragments can be found that bind to a specific pocket of interest on the target, and this information can be used to guide synthesis, especially if additional structural information can be obtained. Herein we describe the NMR based screening that led to the discovery of seven novel inhibitors of the ZipA/FtsZ complex. In conjunction with the NMR studies, the potency of the individual hits was further measured using a fluorescence polarization assay for disruption of the ZipA/FtsZ interaction.¹⁵ Potencies for analogs of the best lead were also determined in hope to establish preliminary structure–activity relationships. In addition, crystal structures of several complexes of ZipA with the leads were obtained and used to further guide a structure-based drug discovery effort. As will be described, the integration of NMR-based screening, biochemical assay, and X-ray crystallography enabled the discovery and validation of low molecular weight hits, the rapid analysis of

structurally related compounds, and an understanding of the interaction of the hits with the target, which helped guide the subsequent rapid optimization of these hits through structure-based design. Given the interactions between ZipA and FtsZ, it would be expected that any inhibitor to this ZipA site would display a hydrophobic nature. However, it is also important to ultimately build in some polar interactions to help increase potency. The introduction of polar groups would have the further advantages of improving ligand solubility and providing consistency in the orientation of the ligand in the binding pocket. While the screening and the primary focus on this work was on the hydrophobic interactions, one of our goals was to look for opportunities where hydrophilic interactions could also contribute to the medicinal chemistry process.

2. Results and discussion

2.1. Compound library selection

The NMR library was composed of 825 compounds selected from the corporate library. Since we desired a structurally diverse set, we chose the compounds such that no two compounds had the same ring scaffold.¹⁶ These compounds were further filtered based on their size, $\text{clog } P$ and by their amenability to being chemically modified. The final distribution of molecular weights of the compounds was between 200 and 250 Da. These small scaffolds were chosen so that they could be rapidly expanded by further chemical synthesis. The expectation that, given their size, the compounds would bind weakly to the target (high μ M to low mM affinity) necessitated the ability for them to be screened at high concentrations. Therefore, compounds with $\text{clog } P$ values < 2.5 were chosen, so they would be likely to have sufficient aqueous solubility.

2.2. NMR experiments

The screening was performed by monitoring the target upon ligand binding by the ^1H – ^{15}N HSQC experiment, using the previously determined¹¹ chemical shifts for ZipA. The observation of the target signals during the screen leads to highly efficient and accurate determination of true binders, as false positives are easily detected by ^1H – ^{15}N HSQC through peak perturbations in uninteresting regions of the protein. In addition, compound aggregation can be monitored easily by taking a 1D spectrum of the mixture prior to the HSQC acquisition. Likewise, protein aggregation is also easily detected by general broadening of HSQC peaks. The 825 compounds selected for the NMR screening library displayed good solubility at a concentration of 500 μ M. NMR samples were composed of a mixture of 6 (or fewer) compounds in the ZipA buffer, and the 1D spectrum of the mixture was acquired. The mixtures were checked first to ensure that the compounds behaved well and did not aggregate in the presence of each other. The 1D spectrum of the compound mixture with ZipA displayed sharp lines, indicative of well-behaved compounds. Spectra were acquired for 140 mixtures. Fifteen mixtures

showed perturbations in the ^1H – ^{15}N HSQC spectrum and these samples were further deconvoluted to test the individual compounds with ZipA. Sixteen compounds were found to bind to ZipA.

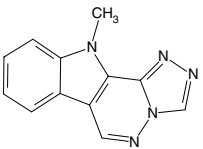
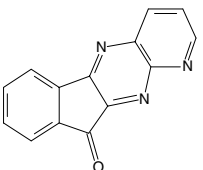
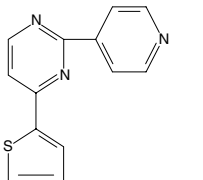
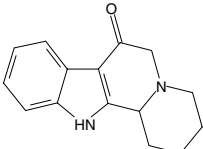
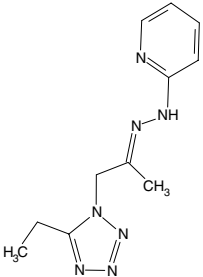
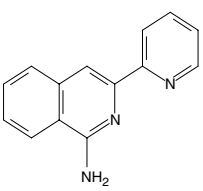
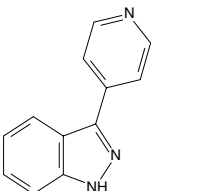
2.3. NMR hits

Table 1 shows the seven compounds that showed perturbations in the ^1H – ^{15}N HSQC peaks corresponding to residues that are involved in the interaction with FtsZ. The other nine compounds interacted with ZipA protein residues that were not in the FtsZ binding pocket, with only few peaks showing perturbation in the ^1H – ^{15}N HSQC spectra, suggesting that the perturbations are not through specific binding to the protein. The seven specific hits also showed a modest inhibition in the fluorescence polarization competition assay of ZipA with a fluorescein-FtsZ peptide, as listed in Table 1. All the hits listed in Table 1 perturbed ZipA HSQC peaks from residues to different extent, depending on their affinity to ZipA. These perturbations changed the chemical shifts of ^1H and ^{15}N resonances about 20–100 Hz, which is expected for such weak binders at the concentrations used. No changes in peak intensities were observed for the HSQC peaks. Compound 4 showed the largest perturbations in the ^1H – ^{15}N HSQC spectrum of ZipA, as displayed in Figure 1. Unfortunately, the HSQC signal for Phe85, one of the key residues involved in the interactions with the compound, was overlapped with three other residues, so it could not be unambiguously determined if its peak shifted upon binding to all hits. Small shifts were observed for the cluster of peaks containing Phe85 resonances. The amide of Phe85 is roughly 10 Å from the ligand ring system, thus it would not be subject to a large chemical shift change due to ring current effects. Not surprisingly, these seven hits are highly lipophilic, as they bind in the hydrophobic patch on ZipA. It is also worth reiterating that these seven compounds come from our small, diverse, lead-like library and thus represent seven different starting points for a medicinal chemistry program. The general scaffolds include pyrimidines, indoles, and aryl indazoles which are all readily amenable to analog preparation.

2.4. X-ray structure of compound 4 and ZipA

A high quality X-ray crystal structure of ZipA with 4 was obtained.^{17,18} The pose of ligand 4 with ZipA has been previously shown,¹⁷ but no details on the interaction were provided. The structure¹⁷ reveals that 4 is binding in the same site that the FtsZ peptide binds, in very close contact with the hydrophobic methyl groups for Val10, Ile12, Ile44, and Ala62 from ZipA. The hexahydroquinolizinone 4 binds to the surface hydrophobic pocket such that Leu372, Ile374, Phe377, and Leu378 of FtsZ can no longer interact with ZipA. MM-PBSA-based calculations¹⁹ suggest that the favorable contributions to the ΔG of binding of 4 arise from the hydrophobic effect, its conformational rigidity, van der Waals interactions, a π -stacking interaction with Phe85 (which forms part of the floor of the ZipA pocket), and very minimal desolvation of polar groups. We were encouraged to observe that ligand 4 formed a hydrogen bond to a water molecule that

Table 1. Hits from the NMR screen of ZipA and their activities in the fluorescence polarization assay

Compound	Structure	Inhibition at 50 $\mu\text{g/ml}$ (%) by fluorescein-FtsZ peptide fluorescence polarization (FP) competition assay
1		61.4
2		23.1
3		24.8
4		62.1
5		7.5
6		20.6
7		35.4

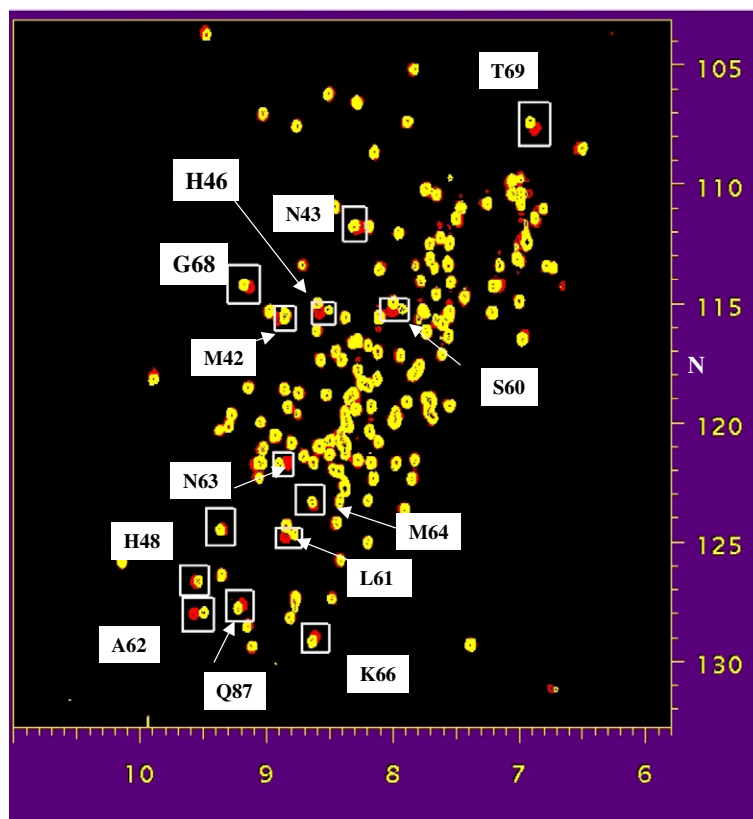


Figure 1. ^1H – ^{15}N HSQC spectrum of 60 μM ZipA (red) and 60 μM ZipA in the presence of 500 μM of compound **4** (yellow). Residues in ZipA perturbed due to binding of the compound are labeled. The amino acid numbering scheme used here for ZipA starts with M1, D2 and ends with A144, which corresponds to M185, D186 to A328 in full-length ZipA.

bridges the carbonyl group of the inhibitor and the backbone carbonyl of Asn63. While this is weak in nature, it did provide a new interaction, importantly a polar one, that could be exploited in the design process. Compound **4** sits in the deepest part of the groove, mostly making contact with residues in the β -strand, and centered in the hydrophobic core of the binding site as can be seen in Figure 2A. The affinity of this compound to ZipA, as determined by HSQC titrations, was found to be around 0.5 mM (data not shown). Thus, if one were to express the equilibrium binding data in terms of the binding interface area, one would obtain a value of $7.6 \text{ cal mol}^{-1} \text{ \AA}^{-2}$ for compound **4** and $5.2 \text{ cal mol}^{-1} \text{ \AA}^{-2}$ for the FtsZ peptide ($K_d = 7 \text{ }\mu\text{M}$ and BSA $\sim 1350 \text{ \AA}^2$); evidence that even this weak small molecule is more efficient in binding than the larger peptide derived from ZipA's natural partner.

2.5. Elaboration of the best hit

In order to further explore the SAR of this hit and potentially identify analogs with a higher affinity, the corporate and commercial collections were searched for structures similar to **4**. Both examples of the linear 6-6-5-6 ring system and other similar ring systems that would afford similar coverage across the hydrophobic cavity were explored. We further sought examples of molecules which, as well as having these hydrophobic interactions, improved on the hydrogen bonding interaction of **4** by having functionality which displaced the

hydrogen-bonded bridging water molecule and formed a direct hydrogen bond to the protein. Eighty-seven compounds were chosen for testing in the FP assay and evaluation by ^1H – ^{15}N HSQC experiments. More than half of the analogs displayed poor solubility upon dissolving in the NMR buffer, preventing the detection of binding. Table 2 displays a subset of these compounds which possessed better solubility and for which perturbations of the residues in ZipA in the FtsZ binding site were observed. All showed only modest activity in the fluorescence assay, with inhibition ranging from 0 to 38% at 5 $\mu\text{g/ml}$. Compounds **9**, **10**, **12**, **17**, **20**, and **21** displayed the largest HSQC perturbations when added to ZipA, suggesting that they were the better binding analogs (data not shown). It is interesting that the fluorescence polarization assay was not able to detect the weak binding to ZipA for many of the analogs for which the HSQC experiment unambiguously showed specific binding to ZipA, demonstrating the high sensitivity of the HSQC experiment. At the concentrations used in this screen, ligands with affinities up to 2 mM could be easily detected.¹³

2.6. X-ray structures of ZipA and analogs of compound **4**

In order to better understand the details of the interactions between analogs of compound **4** and ZipA, co-crystallization experiments of those which showed the largest perturbation in the HSQC spectra were car-

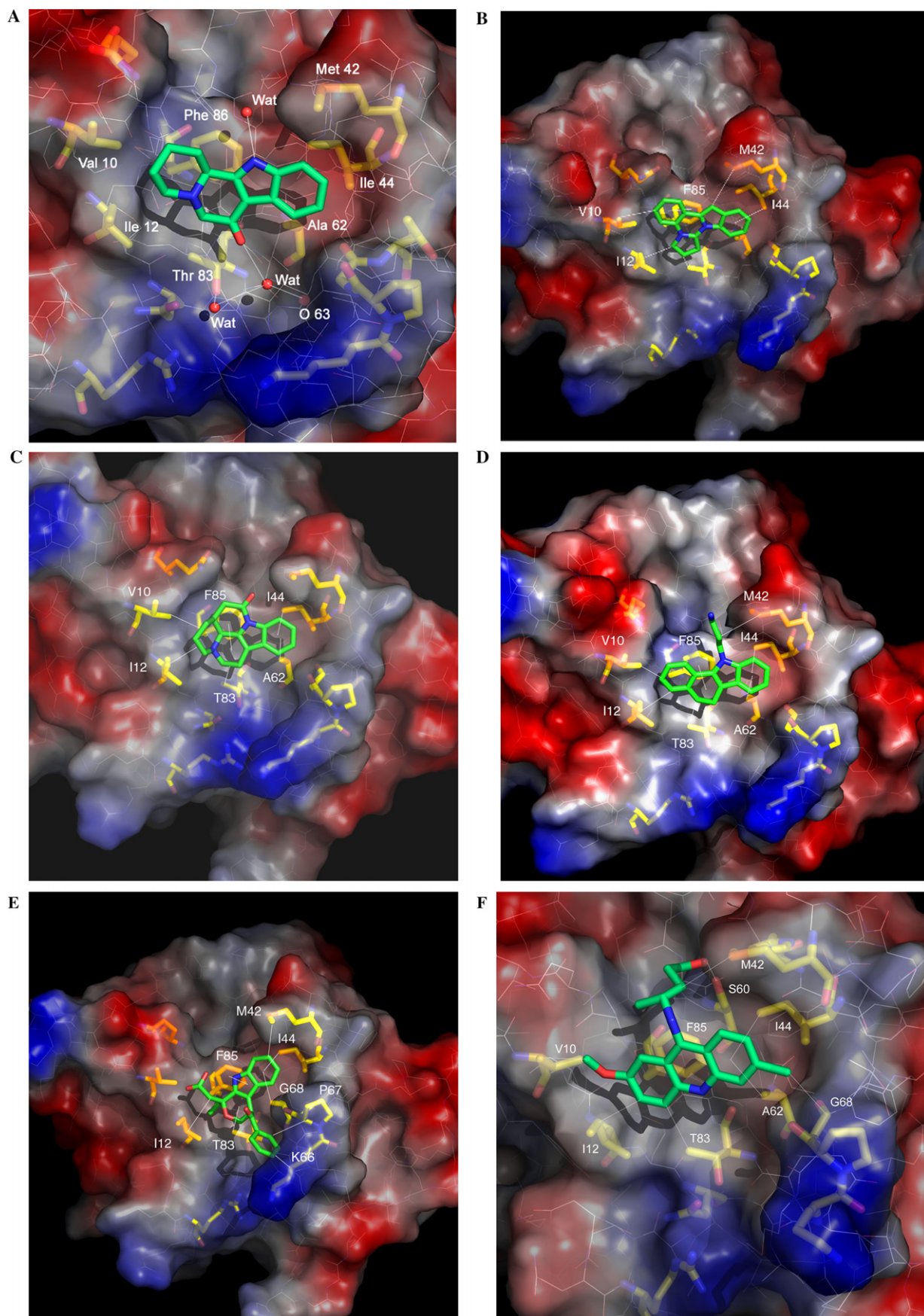


Figure 2. Surface representation of the crystal structure of ZipA (solid surface colored by electrostatic) bound to several inhibitors. Side chains that are within 4 Å of the compounds are connected by a white line. (A) Compound **4**, with water molecules represented by red dots, (B) compound **9**, (C) compound **10**, (D) compound **17**, (E) compound **20**, (F) compound **21**. The interaction of the compounds with ZipA are shown by the yellow side chains in ZipA.

Table 2. Subset analogs of **4** which showed binding by HSQC and their activities in the fluorescence polarization assay

Compound	Structure	Inhibition at 50 $\mu\text{g/ml}$ (%) by fluorescein-FtsZpeptide fluorescence polarization (FP) competition assay
8		25.3
9		38.2
10		n/a
11		0.7
12		−2.1
13		1.7
14		0.7
15		0

Table 2 (continued)

Compound	Structure	Inhibition at 50 $\mu\text{g/ml}$ (%) by fluorescein-FtsZpeptide fluorescence polarization (FP) competition assay
16		−1.5
17		7.9
18		−2.8
19		3.9
20		n/a
21		35.5

ried out. Compounds that were successfully co-crystallized with ZipA (**9**, **10**, **17**, **20**, and **21**) are shown in [Figures 2B–F](#). The side chains of the amino acids making

significant contact with each ligand are highlighted. White lines depict residues that are within 4 Å of the compound. All complexes showed a complimentary match between the core scaffold of each ligand and the shallow pocket of the FtsZ binding region of ZipA. However, there was little or no discernable pattern to the positioning of substituent groups and side chains protruding from the different scaffolds.

As anticipated, compound **9** was also found nestled into the hydrophobic cavity with an orientation similar to that of **4** (Fig. 2B). Our calculations also predict the use of similar contributions to the free energy of binding by compound **9**, with the exception of the enthalpic contribution from a water-mediated hydrogen bond to the surface of ZipA that compound **4** is able to make. Interestingly, two binding modes were observed in the same asymmetric unit for this compound. In both modes, the long axis of the molecule spans the FtsZ binding site and the conjugated π system interacts with Phe85. The similarity of van der Waals interactions observed for these two binding orientations suggests that the two binding modes are not likely to differ in energy (but may arise from small constraints imposed by the crystal lattice). Similarly, the pentacyclic system **10** overlays quite well with compound **4** in the hydrophobic surface cavity. A major pharmacophoric difference, however, is the orientation and location of the carbonyl group, which, in this case, is not making a water-mediated interaction with the ZipA backbone and appears to remain almost completely solvated. Much in the same way, the dihydrocarbazole **17** fills the same hydrophobic cavity as **4**, and does not make any hydrogen bonding interactions with ZipA. It should be noted that the co-structure of compound **17** with ZipA has been reported previously,¹⁷ and similarly to **4**, no details of the interactions were discussed. The alkyl-amine chain extending off the indole nitrogen appears to be almost completely solvent exposed and does not make any additional interactions with the protein. Its free energy of binding is largely driven by the hydrophobic effect, van der Waals interactions, and the stacking interaction with Phe85. Compound **20** was identified by a search of our compound library that aimed to find molecules that displaced or interacted with the bridging water molecule observed in the complex of ZipA with compound **4**. Compound **20** does in fact displace this water molecule, but molecular modeling indicated that it primarily derives its binding energy from its shape complementarity and hydrophobic effect. The ring extension on compound **20** makes additional hydrophobic contacts with Lys66 (Fig. 2E). Acridine **21** was identified by targeting similarly rigid, aromatic systems that could span the hydrophobic cavity of interest. The 6-6-6 acridine ring system overlays quite well with the 6-6-5-6 system of **4**, such that one of the acridine phenyl rings occupies a similar position in the site as the phenyl ring of the indole portion of **4**. The phenyl ring on the opposite side of the acridine system stacks with Phe85. We were delighted to note that the chain protruding from the acridine ring system remains in contact with the ZipA surface, and appears to be making a hydrogen bond from its terminal OH to ZipA's Ser60. This provided a

second polar interaction, in an area of ZipA which does not interact with FtsZ. The total surface area lost upon binding of all these compounds is between ~600 and 730 Å², with compound **21**, owing to the presence of its hydroxybutylamino side chain.

2.7. Potential for finding an inhibitor for the ZipA/FtsZ interaction

The lead obtained from this screen formed the basis for a medicinal chemistry effort to discover potent analogs of compound **4** capable of inhibiting the ZipA/FtsZ interaction and inhibiting bacterial cell division. SAR derived from subsequent investigations of its analogs by both HSQC experiments and crystallography helped guide the effort to increase the potency of binding of **4** to ZipA. Medicinal chemistry efforts were directed at both the derivatization of the lead **4** and replacement of the scaffold of **4** with alternate scaffolds which allowed the introduction of additional side chains.^{17,18,20} The polar interactions observed between the FtsZ peptide and ZipA are not immediately adjacent to the area of the hydrophobic pocket occupied by our ligands, and were not taken as immediate target during our sub-structure searches. However, during later stages of the project, especially during structure optimization, they were taken into consideration.

The crystal structure of compound **21** with ZipA reveals a greater degree of coverage of the FtsZ binding pocket by this compound. So it was reasoned that substituents extending off the indoloquinolizine core of **4** capped with either hydrogen bond donating or hydrogen bond accepting functionality could simultaneously make additional hydrophobic interactions with the FtsZ binding pocket and hydrogen bond interactions with polar amino acid substituents in the periphery of the FtsZ binding pocket. This idea was put to practice,¹⁸ but no significant improvement on the binding potency was observed. Many of the analogs synthesized were found to bind to ZipA by HSQC experiments, but displayed limited solubility. In a subsequent study,¹⁷ analogs of **4** bearing a hydrophobic biaryl side chain capped with a carboxyl group were found to have improved inhibition of ZipA/FtsZ interaction (IC₅₀ ZipA/FtsZ 190–6 μ M). And in a second subsequent study,²⁰ analogs bearing two side chains, one being a water-solubilizing group and one being a hydrophobic group, were also found to exhibit improved inhibition of ZipA/FtsZ interaction (IC₅₀ ZipA/FtsZ 270–3 μ M). These results supported our emerging view that interaction of the ligands with ZipA is dominated by hydrophobic forces and that directing polar interactions between the ligands and protein were either not efficiently accessed or did not significantly contribute to increase in binding energy. The analogs synthesized did not achieve the desired potency and ultimately another lead originating from HTS screening and scaffold hopping efforts was pursued.²¹

Our screening paradigm addressed compound physical properties to a reasonable extent, in particular molecular weight and clogP in the library selection process as

well as solubility and aggregation as part of the NMR screening. However, biological issues such as bacterial cell wall permeability and non-specific protein binding could not be addressed immediately. The process might be further improved by utilizing new generations of libraries filtered by more rigorous physical and biological properties.

3. Conclusions

The discovery of an inhibitor that is able to disrupt a protein/protein interaction with therapeutically useful levels of potency remains extremely challenging.²² In general, protein–protein complexes bury a large area of protein surface and a small molecule inhibitor needs to bind to one protein partner with sufficient affinity to disrupt the complementarity of the binding surfaces. We undertook the challenge to find an inhibitor for the ZipA/FtsZ interaction, where a collection of compounds representing a diverse set of scaffolds were screened for specific binding to the FtsZ binding site of the bacterial protein ZipA, using HSQC experiments. After initial characterization of these compounds by NMR, binding experiments using a fluorescence polarization assay and structural information obtained from X-ray crystallography provided a basis for understanding the structural features of ligand binding to the ZipA pocket. Features common to all of the different ligand-protein complexes involve the presence of π -stacking interactions between the ligands and Phe85, but at the same time showed the variety of different binding orientations available to the ligands in the large, open binding area. Molecular modeling was able to assist in the design of compounds that were a good fit with the protein binding pocket of ZipA but the shallow depth of the pocket and the relative importance of hydrophobic interactions between ligand and protein dominated the complementarity and designing additional binding determinants was challenging. These biological factors ultimately resulted in this process not identifying a compound that could interfere with the interaction of ZipA with FtsZ at a therapeutically relevant level of potency. However, the integration of NMR and X-ray crystallography techniques described here provided complementary information, where real inhibitors were rapidly identified and their structures were quickly obtained, advancing the project to a key decision point at a rapid pace. This interdisciplinary effort represented the first attempt to obtain a ZipA/FtsZ protein/protein inhibitor using rational drug design.

4. Experimental

4.1. Protein expression and purification

ZipA was cloned into a pET vector and expressed in *E. coli*, using minimal media at 37 °C with ¹⁵N ammonium sulfate. The cells containing ZipA were purified according to Moy et al.¹² After the last step of the purification, ZipA was passed through a TSK-G3000SW size-exclu-

sion column, and exchanged into the appropriate buffers.

4.2. NMR experiments

The NMR samples contained ¹⁵N labeled ZipA at ~50–60 μ M, in 50 mM sodium phosphate, pH 5.5, 50 mM potassium chloride, and 2 mM sodium azide, 90% H₂O/10% D₂O, with ~8.5% DMSO (v/v) in the presence of 500 μ M compound, or a mixture of 6 (or less) compounds at 500 μ M each. NMR screening methods are able to identify weak binding, and the concentrations of ZipA and compound were chosen so that we could detect binders with a dissociation constant up to 2 mM. All NMR experiments were acquired on a Bruker Avance 600 spectrometer with a conventional ¹H/¹³C/¹⁵N gradient probe or with a ¹H/¹³C/¹⁵N Bruker cryoprobe system. 1D spectra of the mixture of compounds were acquired to insure that compound mixtures that aggregated were not used in the screen. The ¹H–¹⁵N sensitivity enhanced HSQC was acquired with 48 scans (or 16 scans with the cryoprobe) and 55 complex points. The HSQC spectra were processed with TCL scripts using Principal Component Analysis (PCA) with nmrPipe.²³ The data were displayed with special PCA software. The estimated value of K_d of **4** was obtained via a titration of the compound (from 0.1 to 3.0 mM) to 1 μ M of ZipA. The titration did not reach saturation due to the limit in compound solubility. The chemical shift changes for seven residues (A62, N63, V65, K66, G68, T69, and Q87) were monitored and tabulated according to $\sqrt{(\Delta^1H)^2 + \Delta^{15N/5})^2}$. The K_d was obtained by fitting the compound concentration versus chemical shift changes. The final K_d value was obtained from averaging the individual values obtained for each residue.

4.3. Fluorescence polarization assay

The fluorescence polarization competition assay was performed as described previously.¹⁵ Briefly, the compounds were screened against the ZipA/FtsZ interaction, where the FtsZ peptide was modified by the addition of a fluorophore. The inhibitions were obtained at a fixed compound concentration of 50 μ g/ml.

4.4. X-ray crystallography

ZipA-small molecule inhibitor complexes were formed with a 1.2 M stoichiometric excess of the inhibitor. Co-crystals were prepared essentially as described for crystallization of the free protein.¹¹ Prior to data collection, all crystals were flash cooled in liquid nitrogen at 100 K using 25% ethylene glycol as a cryoprotectant. Diffraction data for the different ZipA/compound complexes were measured in-house using RAXIS IV imaging plate system. The data were processed with DENZO²⁴ and then scaled and merged with SCLALE-PACK.²⁵ The structures were solved by molecular replacement with AMORE²⁵ using one ZipA monomer (pdb code: 1F46) as a search model. Initial models were subjected to iterative cycles of rebuilding and refinement in CNX²⁶ and then used to calculate difference electron density maps, which showed clear densi-

ties for the bound compounds. The final models have good *R*-factors and good geometries according to PROCHECK.²⁷ The X-ray structure coordinates discussed in this paper have been submitted to the Protein Data Bank.

Acknowledgments

We thank Tom McDonagh and Hunter Malason for providing us with ¹⁵N labeled ZipA and Tania Shane for the preparation of protein crystals.

References and notes

- Walsh, C. *Nat. Rev. Microbiol.* **2003**, *1*, 65–70.
- Rothfield, L. I.; Justice, S. S.; Garcia-Lara, J. *Annu. Rev. Genet.* **1999**, *33*, 423–448.
- Rothfield, L. I.; Justice, S. S. *Cell* **1997**, *88*, 581–584.
- Lutkenhaus, J.; Addinall, S. G. *Annu. Rev. Biochem.* **1997**, *66*, 93–116.
- Lutkenhaus, J.; Mukherjee, A. Cell division in *Escherichia coli* and *Salmonella*. In Neidhardt, F. C., Ed.; ASM Press: Washington, DC, 1996; pp 1615–1626.
- Erickson, H. P. *Cell* **1995**, *80*, 367–370.
- Löwe, J.; Amos, L. *Nature* **1998**, *391*, 203–206.
- Liu, Z.; Mukherjee, A.; Lutkenhaus, J. *Mol. Microbiol.* **1999**, *31*, 1853–1861.
- Hale, C. A.; de Boer, P. A. J. *Cell* **1999**, *88*, 175–185.
- Hale, C. A.; de Boer, P. A. J. *J. Bacteriol.* **1999**, *181*, 167–176.
- Moy, F. J.; Glasfeld, E.; Mosyak, L.; Powers, R. *Biochemistry* **2000**, *39*, 9146–9156.
- Mosyak, L.; Zhang, Y.; Glasfeld, E.; Haney, S.; Stahl, M.; Seehra, J.; Somers, W. S. *EMBO J.* **2000**, *19*, 3179–3191.
- Hadjuk, P. J.; Gerfin, T.; Boehlen, J. M.; Haverli, M.; Marek, D.; Fesik, S. W. *J. Med. Chem.* **1999**, *42*, 2315–2317.
- Moore, J.; Abdul-Mana, N.; Fejzo, J.; Lepre, C.; Peng, J.; Xie, X. *J. Synchr. Radat.* **2004**, *11*, 97–100.
- Kenny, C. H.; Ding, W.; Benard, S.; Dushin, E. G.; Sutherland, A. G.; Mosyak, L.; Kriz, R.; Ellestad, G. *Anal. Biochem.* **2003**, *15*, 224–233.
- Nalakantan, R.; Immermann, F.; Haraki, K. *Comb. Chem. High Throughput Screen.* **2002**, *5*, 105–110.
- Sutherland, A. G.; Alvarez, J.; Ding, W.; Foreman, K. W.; Kenny, C. H.; Labthavikul, P.; Mosyak, L.; Petersen, P. J.; Rush, T. S.; Ruzin, A.; Tsao, D. H. H.; Wheless, K. L. *Org. Biomol. Chem.* **2003**, *1*, 4138–4140.
- Jennings, L. D.; Foreman, K. W.; Rush, T. S.; Tsao, D. H. H.; Mosyak, L.; Li, Y.; Sukhdeo, M. N.; Ding, W.; Dushin, E. G.; Kenny, C. H.; Moghazeh, S. L.; Petersen, P. J.; Ruzin, A. V.; Tuckman, M.; Sutherland, A. G. *Bioorg. Med. Chem. Lett.* **2004**, *22*, 1427–1431.
- Rush, R. S.; Manas, E.; Tawa, G.; Alvarez, J. Solvation-based scoring for high throughput docking. In Virtual screening in Drug Discovery; Alvarez, J., Shoichet, B., Eds.; 2005; pp 241–269.
- Jennings, L. D.; Foreman, K. W.; Rush, T. S.; Tsao, D. H. H.; Mosyak, L.; Kincaid, S. L.; Sukhdeo, M. N.; Sutherland, A. G.; Ding, W.; Kenny, C. H.; Sabus, C. L.; Liu, H.; Dushin, E. G.; Moghazeh, S. L.; Labthavikul, P.; Petersen, P. J.; Tuckman, M.; Haney, S. A.; Ruzin, A. V. *Bioorg. Med. Chem.* **2004**, *1*, 5115–5131.
- Rush, T. S.; Grant, J. A.; Mosyak, L.; Nicholls, A. *J. Med. Chem.* **2005**, *48*, 1489–1495.
- Toogood, P. L. *J. Med. Chem.* **2002**, *45*, 1543–1557.
- Delaglio, F.; Grzesiek, S.; Vuister, G. W.; Zhu, G.; Pfeifer, J.; Bax, A. *J. Biomol. NMR* **1995**, *6*, 277–293.
- Otwinowsky, Z. *Data Collection and Processing*. In Sawyer, L., Isaacs, M., Bailey, S. W., Eds.; SERC Daresbury Laboratory: Warrington, UK, 1993; pp 56–62.
- Navaza, Z. *Acta Crystallogr. A* **1994**, *50*, 157–163.
- Brünger, A. T. et al. *Acta Crystallogr. D* **1998**, *54*, 905–921.
- Laskowski, R. A.; Moss, D. S.; Thornton, J. M. *J. Mol. Biol.* **1993**, *231*, 1049–1067.